Feature Selection for Discrimination of Fractionation Levels in Atrial Electrograms

A. Orozco-Duque[1], J.D. Martinez-Vargas[2], D. Novak[3], J. Bustamante[1], and G. Castellanos-Dominguez[2]

Abstract— **Radiofrequency catheter ablation of atrial fibrillation (AF) guided by complex fractionated atrial electrograms (CFAE) is associated with a high AF termination rate in paroxysmal AF, but not in persistent. CFAE does not always identify favorable sites for persistent AF ablation. Studies suggest that only high fractionation level should be used as a target site for ablation. Nonetheless, there are not a standardized criterion to defined fractionation levels. Therefore, a better characterization of the signal is required providing a set of more powerful features that should be extracted from CFAE. Due to the apparent difference among fractionation classes in terms of their stochastic variability, we test time-domain and time-frequency based feature extraction approaches. Also, we carried out the symmetrical uncertainty-based feature selection to determine the most relevant features which improve discrimination of fractionation levels. Obtained results on a tested real electrogram database show that most relevant features in time-domain are related with time intervals and not with amplitudes. Nonetheless, time-frequency features obtained more information from the signal and this representation is likely a better suitable discriminating approach, particularly to detect high fractionated electrograms with a sensitivity and specificity of 83.0% and 93.6%, respectively.**

I. INTRODUCTION

Among cardiovascular diseases, atrial tachyarrhythmias are one of the major causes of morbidity, being atrial fibrillation (AF) the most common type affecting $2\,\%$ of population with increasing incidence. Worse still, AF is a significant and growing expense for health systems.

To study propagation patterns in AF patients, recordings inside the heart chambers using catheter (termed *Atrial electrograms* - EGM) are widely considered. Most clinical electrophysiologists pay attention to complex fractionated atrial electrograms (CFAE), whose ever-changing morphologies, interbeat intervals, and amplitudes are assumed to harbor AF sources. Moreover, several studies have shown that only CFAE signals with high fractional levels are suitable targets for ablation, used to remove fibrillatory substrates [1]. Nonetheless, different fractionation levels and morphologies presents in EGM are not well described, making difficult distinguishing among them [2]. Furthermore, most of the proposed methods to detect CFAE do not discriminate between intermediate and high levels of fractionation EGM [1].

To deal with the above explained restrictions, different approaches have been proposed to discriminate among fractionation levels by using extensive feature sets [3], however, their correlation with arrhythmogenic substrates is still an open issue. Here, to better encode non-stationary behavior of EGM recordings, we propose two different sets of features: one based on time EGM signal descriptors and another is time-frequency-based. Afterward, we select the most relevant features belonging to each set to feed a simple *k-nn* classifier, aimed to distinguish different CFAE levels.

II. METHODS

A. Descriptive time-domain features

CFAE is a low voltage atrial EGM composed by either two deflections or fractionated EGM with a baseline perturbation [4]. Besides, several CFAE has very short cycle length ($<120\,ms$) with or without multiple potentials, where each cycle length is defined as the time between two local activation waves (LAW). Thus, CFAE is calculated by detecting deflections and LAWs over time-domain observations. Particularly, a detection algorithm is given in [5] where near-field potentials are extracted from EGMs, then, LAWs can be detected by applying an adaptive threshold in the "near-field" signal after squaring and moving window integration.

In practice, deflections are searched by detecting pairwise maximum-minimum events representing near and far components of EGM signal, $\boldsymbol{x}\in\mathbb{R}^T$. To this end, we use a zero-crossing detector of the first derivative along the input signal length $T\in\mathbb{N}$. Nonetheless, to avoid noise influence, we propose automatically adjust the detection threshold, $\gamma(i)$, during each *i*-th LAW segment. Specifically, the needed threshold is fixed as $\gamma(m)=\gamma(0)+0.2x_{\max}\ \forall m=1,\ldots,M$ with M the number of LAWs, $x_{\max}$ is the maximum EGM signal value within the LAW interval, and $\gamma(0)$ is the voltage threshold at $t=0$, computed as the root mean square value of $\boldsymbol{x}$ along T and divided by an introduced sensitivity parameter, $a\in\mathbb{R}^+$. The same LAW length is fixed as the window lasting from the middle point of the interval between neighboring i and $i-1$ LAW segments to the middle point of the interval between i and $i+1$ LAW segments.

As a result, derived from the above segmentation procedure, we consider the following set of $n_F=12$ descriptive features shown in Table I where the number of inflection points is calculated using zero-crossing detection along the second derivative.

*This work is supported by COLCIENCIAS project No. 121056933647 and by the project "Plataforma tecnológica para los servicios de teleasistencia, emergencias médicas, seguimiento y monitoreo permanente a los pacientes y apoyo a los programas de promoción y prevención - Eje 2, programa e-salud, convocatoria Regalías", ARTICA, Colombia

[1]Universidad Pontifica Bolivariana, Centro de Bioingeneria, Medellin, Colombia, andres.orozco@upb.edu.co

[2]Universidad Nacional de Colombia, s. Manizales, Signal Processing and Recognition Group.

[3]Department of Cybernetics, Faculty of Electrical Engineering, Czech Technical University in Prague.

978-1-4244-7929-0/14/$26.00 ©2014 IEEE

TABLE I

SUMMARY OF TIME-DOMAIN BASED FEATURES

Index	*Feature*	*Description*
1	AWp	total number of LAW
2	MMp	total number of maxima points
3	MMp mean	mean of max-min pairs intervals
4	BC sd	stand. dev. of max-min pairs intervals
5	Infl.	Number of inflection points
6	AW sd	standard deviation of intervals between LAWs
7	AW mean	mean of intervals between LAWs
8	LAW/MMp	(LAWs)/(max-min points)
9	MMa mean	mean of max-min pair amplitude
10	MMa sd	standard deviation of max-min pair amplitude
11	LAWa mean	mean of amplitudes of LAWs
12	LAWa sd	standard deviation of LAWs amplitudes

B. Features extracted from time-frequency representation

To analyze non-stationarity of signals, we employ the continuous wavelet transform (CWT) quantifying similarity between a given EGM time-series $\boldsymbol{x}$ and a basis function set $\boldsymbol{\psi}(\tau, b)\in\mathbb{R}^T$, using the inner product based decomposition:

$$s(t,b) = \langle \boldsymbol{x}, \boldsymbol{\psi}^*((\tau - t)/b)\rangle, \tag{1}$$

where * denotes the complex conjugate, $b\in\mathbb{R}^+$ is the scale, and $\tau\in\mathbb{R}^+$ is the support interval of analysis. Consequently, by varying the wavelet scale b and translating along the localized time index t, we can construct scale representations pointing out on spectral variations along the time.

C. Symmetrical uncertainty-based feature selection

Relevance analysis distinguishes those salient features (termed as *relevant features*) better representing the subjacent physiological phenomena, in terms of an a priori fixed measure of evaluation (*relevance measure*). Consequently, feature selection aims to reject those variables that have negligible representing abilities.

However, due to clear difference among fractionation levels in terms of their stochastic variability, we use as the relevance measure its *Symmetrical uncertainty*, $\rho\in\mathbb{R}^+$, that for a given feature, $\boldsymbol{\xi}\in\mathbb{R}^{n_O}$, $n_O\in\mathbb{N}$, is defined as follows [6]:

$$\rho(\boldsymbol{\xi}|C) = 2\frac{H(\boldsymbol{\xi}) - H(\boldsymbol{\xi}|C)}{H(\boldsymbol{\xi}) + H(C)}, \tag{2}$$

where $H(\cdot)\in\mathbb{R}^+$ is the entropy estimated over the total number of observations, $n_O\in\mathbb{N}$. Likewise, $H(\boldsymbol{\xi}|C)$ is the conditional entropy of the conditional distribution of $\boldsymbol{\xi}$, given the explained below class label collection $C = \{c_0, c_{1+2}, c_3\}$.

III. EXPERIMENTAL SET-UP

A. Database acquisition and preprocessing

To validate the proposed training approach, we use the data collection provided by "*Staedtisches Klinikum Karlsruhe*"* that holds a set of n_O=429 recordings acquired after pulmonary vein isolation using a multipolar circular catheter. All patients were indicated for radiofrequency ablation AF. Each signal was recorded at $1.2\,kHz$ sampling rate lasting $1.25\,s$ and bandpass filtered with a $[30, 250]\,Hz$ bandwidth. Then, the baseline wander and high noise were removed using the wavelet-based method described in [7]. Every recording was independently annotated according its morphology by two different electrophysiologists and only signals with the same identification were considered. Information about AF condition or specific arrhythmogenic substrates were no considered in the annotation process. We split the whole training set into the following physiological classes ($c_i\subset C$): 153 recordings are labeled as Non-fractionated EGM (noted as c_0), 223 signals (noted as c_{1+2}) regarding mild and intermediate fractionation levels as labeled in [7], and 53 signals are related to the high (c_3) class. Fig. 1 shows examples of the considered CFAE levels.

*www.klinikum-karlsruhe.com

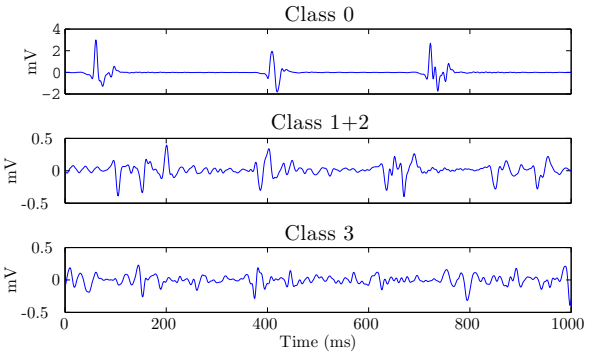

Fig. 1. Examples of the considered EGM recording classes: Fractionation level 0 (labeled as c_0), levels $1\cup 2$ (c_{1+2}), and level 3 (c_3).

B. Feature extraction from EGM recordings

a) Calculation of Time-domain based features: To compute explained above descriptive features and to extract the near field activation, we calculate three fine scales of the Continuous Wavelet Transform using the Mexican-hat mother wavelet. Besides, to accomplish segmentation of near field potentials (see Fig. 2) we carry out detection of LAWs using the integration window and adaptive threshold proposed by Pan and Tompkins. Heuristically, we adjust the value of integration window equals to 40 samples, exceeding the LAW width. In turn for detection of max-min points, the needed threshold sensitivity parameter is fixed as a=3, in accordance to a used Fisher's discriminant ratio-based optimization procedure. Hence, the feature matrix $\boldsymbol{\Xi_1}\in\mathbb{R}^{n_O\times n_F}$ stands for the set of estimated descriptive parameters, where n_F is the number of extracted features.

b) Calculation of time-frequency based feature set: CWT-based characterization of EGM signals is also considered as discussed in [5]. To this, we use the Daubechies-4 mother wavelet for which the number of scales is heuristically fixed as 128. Thus, we extract from each recording a single *t-f* representation, $\boldsymbol{S}(t,f)\in\mathbb{R}^{T\times F}$, holding T=1500 time samples and F=128 frequency or scale points. Then, a *t-f* feature supermatrix $\boldsymbol{\Xi_2}\in\mathbb{R}^{n_O\times TF}$ is obtained by vectorizing each estimated *t-f* representation.

C. Features selection based on analysis of relevance

We carry out relevance analysis based on Eq. (2) that, for each observation, yields a feature vector holding those characteristics whose relevance value is larger than an a priori given threshold $\epsilon \in \mathbb{R}^+$. For the time-domain based features, a single value of relevance is calculated for each feature, obtaining a relevance vector $\boldsymbol{\rho} \in \mathbb{R}^{n_F}$, as shown in Fig. 3(a). In case of the *t-f* based features, a relevance value is computed for each point of the *t-f* representation (Right panel of Fig. 3(b)) that is further averaged over the time-axis to get a relevance vector $\boldsymbol{\rho}_{\boldsymbol{rF_{su}}} \in \mathbb{R}^{F}$. Therefore, we choose the most relevant scales through the *t-f* representations.

The tuning procedure of the number of relevant features for each extraction approach is carried out using a simple *k*-nn classifier following the commonly known cross-validation

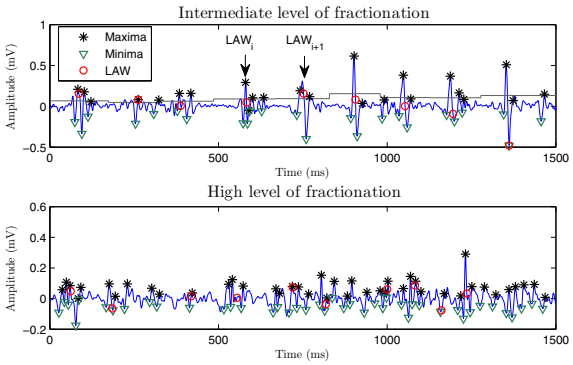

Fig. 2. Sample of EGM segmented signals. Note that not all maximum-minimum pair correspond to a LAW, mainly, in high fractionation signals.

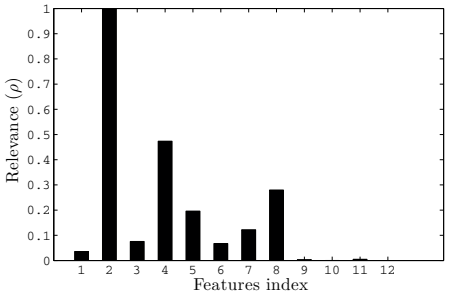

(a) Relevance of time-domain based features

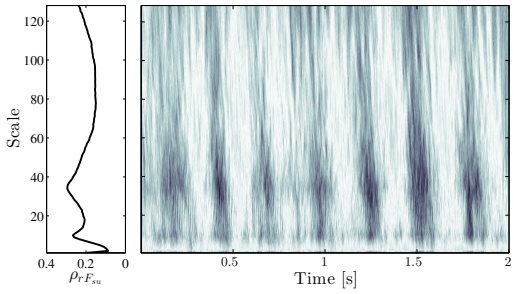

(b) Relevance of *t-f* based features

Fig. 3. Symmetrical Uncertainty measured over each set of features.

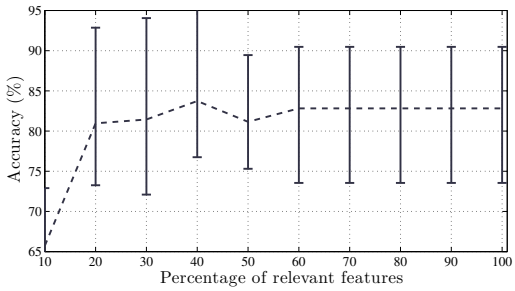

(a) Time-domain based features

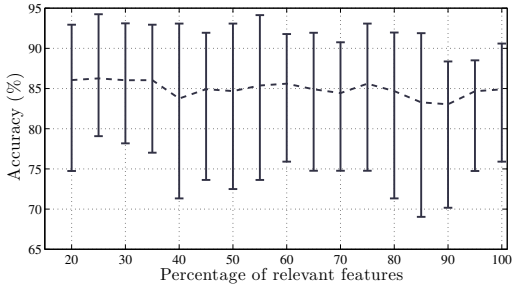

(b) *t-f* based features

Fig. 4. Tuning the number of relevant features, mean and std values over 10 runs are presented. a) Maximum accuracy is reached with 40% of the time-domain based features and b) with 25%of the *t-f* based features.

scheme (i.e., 10-folds). The number of neighbors is set empirically by including all the feature space. Namely, we set k=3 for both feature extraction approaches. Thus, we set the threshold ϵ to overcome a certain percentage of the relevant features. In turn, we stepwise increase from 20% to 100% by 10% steps for the time-domain based feature set, and with steps of 5% for the *t-f* based feature set. Lastly, we accomplish the well-known dimension reduction approach two-dimensional principal component analysis (2D-PCA) to reduce the high-dimensional feature space obtained using the *t-f* based approach. In this case, we set empirically the number of components (in rows and columns) as n_c=25. Fig. 4 shows values of the mean and standard deviation averaged over the 10 folds estimated for tuning the number of relevant features in both approaches (upper panel –the time-domain based features, and lower panel – the *t-f* features).

Overall, according to the results shown in Fig. 4(a), we select the 40% of the most relevant features (corresponding to features 2, 4, 5 and 8 in Table I) for the time-domain based features. For the *t-f* based features, we also select the 25% of the most relevant scales bands (i.e., 32 scales), see Fig. 4(b). Therefore, we get a set holding 80 features after 2D-PCA-based dimension reduction is carried out.

Once all the parameters are tuned by maximizing the average accuracy of class separation, the final results are obtained as the sensitivity and specificity for each class as shown in Table II. It must be quoted that for the sake of comparison, we use the nonlinear statistic Approximate Entropy feature set (noted as *ApEn*) that quantifies signal complexity and turns to have positive relationship to the

degree of fractionation, as discussed in [8] where the needed parameters for their computation are adjusted as m=3 and r=0.38. Notation m stands for embedded dimension and r is a certain sensitivity-to-noise threshold.

TABLE II

PERFORMANCE ACHIEVED BY EACH CONSIDERED FEATURE SET

	ApEn	
Class	S_e (%)	S_p (%)
C_0	85.79±0.10	94.13±0.05
C_{1+2}	83.87±0.04	81.08±0.10
C_3	61.33±0.21	93.92±0.04
CT	69 [*ms*]	
	time-domain set	
Class	S_e (%)	S_p (%)
C_0	87.50±0.11	94.93±0.05
C_{1+2}	**88.36±0.06**	80.01±0.07
C_3	50.00±0.16	**95.72±0.03**
CT	0.9 [*ms*]	
	t-f set	
Class	S_e (%)	S_p (%)
C_0	**89.71±0.08**	**95.63±0.06**
C_{1+2}	85.16±0.08	**89.40±0.07**
C_3	**83.00±0.12**	93.63±0.06
CT	1400 [*ms*]	

Computational time (CT) is computed using `Matlab` environment in a PC with Intel Core i7 processor and 6 GB RAM.

IV. DISCUSSION AND CONCLUSION REMARKS

To differentiate among atrial EGM fractionation levels, we compare three different feature extraction approaches: time-domain, *t-f* domain, and non-linear features. Then, we select the most relevant features per set to train a *k*-nn classifier. As feature selection approach, we use a concrete supervised relevance measure based on the entropy. In this way, we can get the features that best discriminate among classes. Nevertheless, two issues must be considered, namely: *i*) performance strongly depends on how accurate the training set labeling is. In the case of biosignals, this procedure are very subjective to the medical criterion, and *ii*) about the high fractionated signals, time-domain analysis based in LAW intervals is difficult. As a result, obtained results show that *t-f* based features, where the measure does not consider any relationship between LAW segments, are suitable for separating among different fractionation levels. In turn, Fig. 3(b) shows two peaks of relevance around scales, numbered as 10 and 34, that correspond to frequencies close 25 and 86 Hz, respectively. Nevertheless, further studies are needed to verify the physical interpretation of those frequency bands.

Fig. 3(a) shows assessed relevance of the time-domain based features, where highest values of $\boldsymbol{\rho}$ correspond to the total number of maxima points and to time intervals between max-min points. This behavior can be explained because of the CFAE definition that is based on the deflection number within each LAW segment, which holds a direct relationship to maxima and minima points. Also, the LAW and max-min pair amplitude features have the lowest relevance. In bipolar EGM, this fact may be explained since amplitudes are influenced by the action potential propagation direction relative to electrode position.

In this study, we consider two main classification issues: Discrimination of non-CFAE recordings c_0, and discrimination between intermediate and high level fractionation. All the obtained results are summarized in Table II. In the former problem, we did not find significant differences among the three feature sets that also can be compared with the state of the art approaches [9]. In the later case, the time-domain based features achieve high sensitivity values to discriminate recordings belonging to c_{1+2}, but low sensitivity values to detect c_3 recordings. This behavior may be explained because time-domain features are based in a segmentation process; however this class (c_3) is characterized by continuous activity where segments are not apparent, even for physicians [2]. Similar results are achieved with the non-linear feature.

Lastly, we remark that the levels of sensitivity achieved by the *t-f* based features overcome results with the other proposed characterization approaches. This fact suggests that CWT based features are able to capture non-stationary information associated with high fractional signals. Despite the promising results obtained by the *t-f* based features, it must be quoted that this characterization requires significantly most computation time, which can be seen as a drawback of this approach.

The use of relevant features to discriminate EGM fractionation levels and morphologies can improved the localization of target site for ablation based in CFAE. As a future work, we propose to use a combination of classifiers to take advantage of properties supplied by the different characterization methods under consideration in terms of improving discrimination among CFAE levels.

REFERENCES

[1] K. Nademanee, "Mapping of complex fractionated atrial electrograms as target sites for af ablation," in *Conf Proc IEEE Eng Med Biol Soc*, 30 2011-sept. 3 2011, pp. 5539 –5542.

[2] O. Berenfeld and J. Jalife, "Complex fractionated atrail electrograms is this the beast to tame in af," *NIH Public Access*, vol. 4, no. 4, pp. 426–428, 2011.

[3] N. Navoret, S. Jacquir, G. Laurent, and S. Binczak, "Detection of complex fractionated atrial electrograms using recurrence quantification analysis," *IEEE Trans. Biom. Eng.*, vol. 60 (7), pp. 1975–82, 2013.

[4] K. Nademanee, E. Lockwood, N. Oketani, and B. Gidney, "Catheter ablation of atrial fibrillation guided by complex fractionated atrial electrogram mapping of atrial fibrillation substrate," *Journal of Cardiology*, vol. 55, no. 1, pp. 1–12, Jan. 2010.

[5] R. Houben, N. de Groot, and M. Allessie, "Analysis of fractionated atrial fibrillation electrograms by wavelet decomposition," *Biomed. Eng., IEEE Trans. on*, vol. 57, no. 6, pp. 1388 –1398, june 2010.

[6] J. Martinez-Vargas, J. Godino-Llorente, and G. Castellanos-Dominguez, "T-f based feature selestion for discrimination of non-stationary biosignals," *EURASIP J. on Adv. in Signal Proc.*, 2012.

[7] C. Schilling, "Analysis of atrial electrograms," *Karlsruhe Transactions on Biomedical Engineering*, vol. 17, 2012.

[8] A. Orozco-Duque, J. Ugarte, C. Tobon, J. Saiz, and J. Bustamante, "Approximate entropy can localize rotors, but not ectopic foci during chronic atrial fibrillation: A simulation study," in *Computing in Cardiology*, Sept 2013, pp. 903–906.

[9] R. J. Hunter, I. Diab, G. Thomas, E. Duncan, D. Abrams, M. Dhinoja, S. Sporton, M. J. Earley, and C. Schilling, "Validation of a classification system to grade fractionation in atrial fibrillation and correlation with automated detection systems," *Europace*, vol. 11(12), pp. 1587–96, 2009.